ORIGINAL ARTICLE

On the analysis of burst-assembly delay in OBS networks and applications in delay-based service differentiation

José Alberto Hernández · Javier Aracil · Víctor López · Jorge López de Vergara

© Springer Science+Business Media, LLC 2006

Abstract In Optical Burst Switching (OBS), packets travel through the network core as part of longer-size optical bursts, which do not suffer electronic conversion until they reach an eggress point. Typically, such optical bursts comprise tens or hundreds of packets, which are assembled/deassembled at border nodes. During the burst-formation process, each arriving packet must wait until the final burst is complete, which clearly adds an extra delay on each packet in the burst, especially on those arriving earlier. However, such burst-assembly delay may be excessive for the appropriate performance of certain applications, mainly real-time interactive ones. This work's findings are twofold: first, it characterises the burst-assembly delay distribution of each packet in a burst arisen by the main assembly algorithms found in the literature; and, second, it introduces a new burst-assembly strategy that takes into account the particular delay constrains of packets in the formation of optical bursts, along with a detailed study of its properties.

Keywords Optical Burst Switching · Burst-assembly delay analysis · Burst-assembly delay differentiation

Introduction

The Optical Burst Switching (OBS) approach for the design of high-speed operation Internet backbones over

J. A. Hernández (✉) · J. Aracil · V. López · J. L. de Vergara
Networking Research Group, Universidad Autónoma de Madrid, Madrid, Spain
e-mail: Jose.Hernandez@uam.es

Wavelength Division Multiplexed (WDM) network infrastructures has been recently proposed as a solution for the ever-increasing demand of bandwidth capacity [16,20]. In such backbone networks, ingress nodes accumulate incoming packets and generate large-size optical bursts, which are treated optically over the network core.

Clearly, a good understanding of the burst generation process, that is, the burst-assembly algorithms implemented at core nodes, is crucial in determining meaningful network performance measures and further designing and engineering OBS networks [7]. For instance, the size characteristics of optical bursts clearly impact on the probability of finding available time-slots at intermediate nodes at which bursts are to be scheduled [19,10]. Also, the design of the burst-assembly algorithm determines the level of link utilisation [3].

Typically, the process of burst assembly, often referred to as "burstification", follows one of the following policies: size-based [18], time-based [8] and mixed-based [1,21]. The former strategy consists of generating fixed-size bursts, thus gathering input packets until such targeted burst-size is reached. Time-based algorithms assemble input packets for a certain amount of time, which is controlled by a given assembly timer, and generates the optical burst only when such timer expires. Finally, the mixed-based policy combines the two strategies above and generates the optical burst as soon as the time or the size constrain is met, whichever occurs first.

Previous studies have analysed in detail the burst-assembly process, mainly focusing on the characterisation of outgoing burst sizes [14], the burst interdeparture times [5,15], its impact on different aspects of global network performance, such as link utilisation and

blocking probability at intermediate nodes [2,24], or a combination of some of these aspects. Other subjects of interest regarding the burstification process have included the study of the smoothing effect caused on the incoming traffic burstiness [5,8,21,22], the influence of self-similarity [11] and the impact of the burst-assembly process on TCP performance [1,23,26].

However, to the best of our knowledge, only a few studies have paid attention to the actual burst-assembly delay distribution experienced by the packets in a given optical burst and its characterisation [2,25]. For instance, in Zapata et al. [25], only the maximum and average delay values are studied, but no other metrics, such as the variance, nor the actual delay distribution, are derived. Rodrigo de Vega et al. [5] take one step further in the analysis of burst-assembly delay and compute the delay of the first packet in the burst, but do not mention the delay suffered by each of the other packets in that burst. Similarly, Choi et al. [2] study the average burst inter-departure times. Hence, such studies only provide a few statistical metrics of such burst-assembly delay, but, as far as we are concerned, there is no detailed study on the probability distribution of the burst-assembly delay suffered by each packet in an optical burst.

Indeed, the characterisation of such burst-assembly delay probability distribution is key when dealing with interactive applications, such as videoconferencing, Internet telephony and online gaming. Such applications typically constitute only a small portion of the total traffic, and have tight delay-requirements to optimally perform. Accordingly, if not designed carefully, the extra delay added during the burst-assembly process may exceed the maximum delay value tolerated by that application. This problem has been traditionally addressed by assembling packets with the same QoS requirements together [13]. However, if the input rate of such delay-constrained traffic is low and the delay requirements of that particular class are tight, typical assembly algorithms *dispatch bursts with small sizes*. A possible solution to this problem consists of assemblying packets with different delay requirements together, and adjusting the parameters of the assembly algorithms to meet the delay constrains of the packets with the highest priority in the burst.

This work's contribution is twofold: first, it aims to analyse in detail the burst-assembly delay suffered by incoming packets at border OBS nodes under the most common burst-assembly policies found in the literature, along with a comparison between them; and second, it proposes two algorithms for assemblying packets with different delay constrains and analyses the characteristics of the resulting optical bursts.

The reminder of this work is organised as follows: "Burst-assembly process revisited" section analyses in detail the structure and probability distribution of burst-size and packet-delay produced by each burst-assembly algorithm. "Burst-assembly algorithms with service differentiation" presents two delay-constrained burst assembly algorithms, and studies its characteristics and features. Finally, "Summary and conclusions" summarises the main findings and possible further studies arising from this work.

Burst-assembly process revisited

Burst-assembly algorithms are typically employed at ingress OBS nodes, which play the crucial role of bridging traffic towards the all-optical network infrastructure. Essentially, ingress nodes accumulate incoming packets from the outside electrical plane and generate optical bursts of tens or hundreds of packets following a time and/or size policy. To analyse the size and assembly delay characteristics of each burst-assembly algorithm, the forthcoming study shall assume that incoming packets arrive following a Poissonian basis. This assumption has been extensively considered in the optical networks literature [3,5,7,17,18,21] and is gaining in importance among the network research community after the recent studies on network traffic measurements [9,12].

For notation purposes, let $x_i, i = 1, \ldots, N - 1$ refer to the time elapsed between the ith and the $i + 1$th packet arrivals, as shown in Fig. 1. Clearly, under Poissonian arrivals, such interarrival times are negative exponentially distributed with parameter λ.

Essentially, burst-assembly algorithms accumulate traffic until a fixed number of packets or bytes have arrived ($S_{\max}$ condition) and/or the first incoming packet has waited a given amount of time ($T_{\max}$ condition). We shall refer to N as the random variable that represents the number of packets fitting in a burst under the conditions above, and to $d_i, i = 1, \ldots, N$ as the burst-assembly delay suffered by the ith packet in such burst. Clearly, $d_i = \sum_{j=i}^{N-1} x_j$.

For simplicity, all incoming packets shall be assumed equally sized. Finally, it is worth remarking that the
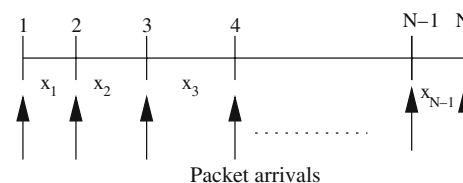

Fig. 1 Packet interarrival times (notation)

amount of packets gathered by any border node within time t is given by:

$$\mathbb{P}(N = n) = \frac{(\lambda t)^{n-1}}{(n-1)!} e^{-\lambda t}, \quad n = 1, 2, \ldots \quad (1)$$

which avoids the case $n = 0$ since all bursts must have at least one packet in it, obviously.

The following section provides deep analysis of the bursts' main features i.e., size structure and burst-assembly delay, obtained by the three typical burst-assembly algorithms: size-based ("Size-based algorithms" section), time-based ("Time-based algorithms" section) and mixed-based ("Mixed-based algorithms" section) algorithms.

Size-based algorithms

Size-based burst-assembly algorithms accumulate packets until the total size of the aggregated traffic reaches a given value, namely $S_{\max}$ or S bytes or packets. Since all incoming packets are assumed to have the same size, then a burst is ready when a number of $S_{\max}$ packets have arrived at the network edge. Thus, the burst-size distribution is constant with value $S_{\max}$ and $\mathbb{P}(N = n) = \delta(n - S), n = 1, \ldots, S$ where $\delta(\cdot)$ is the Dirac delta function.

This algorithm outputs bursts with average-size $E[N] = S_{\max}$ and variance $Var[N] = 0$. According to this, by tuning the $S_{\max}$ parameter in the burstification process, border nodes can size the outgoing bursts, for instance, on attempts to adequately fit them in the forthcoming core nodes scheduler. This is an important feature of size-based burst assembly algorithms.

Concerning the burst-assembly delay suffered by each packet in the burst, the following lemma states its probability distribution:

Lemma 1 *The probability density function $f_{d_i}(d)$ of the burstification delay, d_i, experienced by the ith packet $(i = 1, \ldots, S)$ in the burst follows a Gamma distribution with parameter λ and $S - i$ degrees of freedom, that is:*

$$f_{d_i}(d) = \Gamma_d(S - i, \lambda)$$
$$= \frac{\lambda^{S-i} d^{S-i-1}}{(S-i-1)!} e^{-\lambda d}, \quad i = 1, \ldots, S, \quad d \geq 0 \quad (2)$$

where $\lambda = 1/EX$ is the input traffic rate (EX being the average time of packet interarrivals), and S is targeted burst size.

Proof Eq. 2 arises directly from the fact that $d_i = \sum_{j=i}^{S-1} x_j \sim \Gamma(S - i, \lambda)$, since $x_j \sim \exp(\lambda)$ for $j = i, \ldots, S - 1$ □.

It is worth noting that the probability distribution above has the following mean and variance values:

$$E[d_i] = \frac{S - i}{\lambda} \quad (3)$$

$$Var[d_i] = \frac{S - i}{\lambda^2} \quad (4)$$

which provides the ith packet's delay mean and variance. Clearly, the value $E[d_1] = \frac{S_{\max} - 1}{\lambda}$ is not only the average delay experienced by the first packet, but also gives the average burst-formation time.

Time-based algorithms

Time-based burst assembly algorithms accumulate packets on a time basis. Basically, the first packet arrival triggers the so-called assembly-timer and, after this, incoming packets are aggregated together until the assembly-timer reaches a given threshold value, namely $T_{\max}$ or just T. When so, the optical burst is generated, and the assembly-timer is reset to zero until a new packet arrival starts it.

Under Poissonian packet arrivals with input rate λ, the size of the ouput bursts follows the distribution given in Eq. 1 evaluated at $t = T$:

$$\mathbb{P}(N = n) = \frac{(\lambda T)^{n-1}}{(n-1)!} e^{-\lambda T}, \quad n = 1, 2, \ldots \quad (5)$$

with the following mean and variance values:

$$E[N] = \lambda T + 1 \quad (6)$$
$$Var[N] = \lambda T \quad (7)$$

The analysis of the burst-assembly delay is slightly more complicated than in the $S_{\max}$ algorithms. Basically, the fact that time-based algorithms output variable size bursts, makes difficult the task of computing the ith packet delay, since the burst may have a size $n < i$ packets. Nevertheless, the appendix section "Burst-assembly process revisited" provides the probability distribution of the ith packet delay, assuming a total of n packet arrivals within the interval $[0, T]$. The reader is encouraged to refer to such appendix for further details.

With such result, the following lemma states the actual burst-assembly delay distribution of the ith packet regardless of the actual number of packets comprising the burst.

Lemma 2 *The probability density function $f_{d_i}(d)$ of the burst-assembly delay d_i, $i = 1, 2, \ldots$, experienced by the ith packet in the burst follows a truncated Gamma*

distribution evaluated at $T - d$, with parameter λ and $i - 1$ degrees of freedom, that is:

$$f_{d_i}(d) = \Gamma_{T-d}(i-1, \lambda)$$
$$= \frac{\lambda^{i-1}(T-d)^{i-2}}{(i-2)!}e^{-\lambda(T-d)}, \quad i = 2, \ldots, \quad d_i \leq T$$
$$d_1 = T \quad a.\,s. \tag{8}$$

where $\lambda = 1/EX$ refers to the input traffic rate.

Proof Lemma 4 in the appendix section "Burst-assembly process revisited" gives the delay pdf of the ith packet assuming the burst contains up to $n \geq i$ packets, that is, $f_{d_i|n}(d)$. To compute the delay distribution of the ith packet in any burst with at least i packets, it is necessary to add the probabilities of all cases. This is:

$$f_{d_i}(d) = \sum_{n=i}^{\infty} f_{d_i|n}(d)\mathbb{P}(n)$$
$$= \sum_{n=i}^{\infty} \frac{n!}{(n-i+1)!(i-2)!}\left(\frac{d}{T}\right)^{n-i+1}$$
$$\times \left(\frac{T-d}{T}\right)^{i-2}\left(\frac{1}{T}\right)\frac{(\lambda T)^n}{n!}e^{-\lambda T}$$
$$= \frac{e^{-\lambda T}(T-d)^{i-2}}{(i-2)!}\sum_{n=i}^{\infty}\lambda^n\frac{d^{n-i+1}}{(n-i+1)!}$$
$$= \frac{\lambda^{i-1}e^{-\lambda T}(T-d)^{i-2}}{(i-2)!}\sum_{n=i}^{\infty}\frac{(\lambda d)^{n-i+1}}{(n-i+1)!}$$
$$= \frac{\lambda^{i-1}(T-d)^{i-2}}{(i-2)!}e^{-\lambda(T-d)} \tag{9}$$

$\square$

Therefore, the mean and variance of the ith packet delay is given by:

$$E[d_i] = T - \frac{i-1}{\lambda} \tag{10}$$

$$Var[d_i] = \frac{i-1}{\lambda^2} \tag{11}$$

and the burst-assembly delay suffered by any packet in the burst never exceeds the time-threshold value T.

Finally, it is also worth remarking that, for those cases with $i > n$, the delay is obviously null. The amount of cases at which this event occurs is given by:

$$\sum_{n=0}^{i-1}\frac{(\lambda T)^n}{n!}e^{-\lambda T} = \frac{\Gamma_{inc}(i, \lambda T)}{(i-1)!} \tag{12}$$

where Γ_{inc} refers to the upper incomplete gamma distribution function.[1]

---

[1] Upper incomplete gamma function $\Gamma_{inc}(n, x) = (n-1)!\, e^{-x}\sum_{k=0}^{n-1}\frac{x^k}{k!}$

Mixed-based algorithms

Time and size mixed-based algorithms constitute a combination of the two designs studied above. The burst-assembly algorithm considers a burst is complete when either the accumulated traffic volume reaches the size threshold S_{max} or the burst-assembly timer expires, i.e., T_{max}, whichever occurs first.

According to this, the burst has a size of $N = n$ packets given by:

$$N = \begin{cases} n, & \text{if } n < S_{max} \\ S_{max}, & \text{otherwise} \end{cases} \tag{13}$$

To compute the average burst size, we must take into account the two cases above, i.e., the cases at which the burst is completed due to the S_{max} and T_{max} conditions:

$$E[N] = \sum_{n=0}^{S-1}(n+1)\frac{(\lambda T)^{n-1}}{(n-1)!}e^{-\lambda T} + S\sum_{n=S}^{\infty}\frac{(\lambda T)^{n-1}}{(n-1)!}e^{-\lambda T}$$
$$= S + (\lambda T)\frac{\Gamma_{inc}(S-1, \lambda T)}{(S-2)!} + (1-S)\frac{\Gamma_{inc}(S, \lambda T)}{(S-1)!} \tag{14}$$

where $\Gamma_{inc}(n, x)$ is the upper incomplete gamma function, described before.

The burst-size variance is given by $Var[N] = E[N^2] - (E[N])^2$, where $E[N^2]$ is obtained by:

$$E[N^2] = \sum_{n=0}^{S-1}(n+1)^2\frac{(\lambda T)^{n-1}}{(n-1)!}e^{-\lambda T}$$
$$+ S^2\sum_{n=S}^{\infty}\frac{(\lambda T)^{n-1}}{(n-1)!}e^{-\lambda T}$$
$$= (\lambda T)^2\frac{\Gamma_{inc}(S-2, \lambda T)}{(S-3)!}$$
$$+ 3(\lambda T)\frac{\Gamma_{inc}(S-1, \lambda T)}{(S-2)!} + \frac{\Gamma_{inc}(S, \lambda T)}{(S-1)!} \tag{15}$$

Finally, the burst-assembly delay experienced by the ith packet in the burst takes an expression given by a combination of the results in the sections above. The following lemma states this result.

Lemma 3 *The probability density function $f_{d_i}(d)$ of the burst-assembly delay d_i experienced by the ith packet in a burst generated following a time and size mixed-based policy is given by the following probability distribution:*

$$f_{d_i}(d) = \Gamma_{T-d}(i, \lambda)\frac{\Gamma_{inc}(S-i, \lambda d)}{(S-i-1)!}$$
$$+ \Gamma_d(S-i, \lambda)\left(1 - \frac{\Gamma_{inc}(i, \lambda(T-d))}{(i-1)!}\right),$$
$$i = 1, \ldots, N, \quad d \geq 0 \tag{16}$$

Proof For simplicity, we shall split the proof into two cases: (1) The case $n > S$ which represents the cases

at which the $S_{\max}$ condition is met first; and, (2) the case $n < S$ whereby the burst is assembled due to timer expiration.

(1) If $n > S$:

$$\sum_{n=S}^{\infty} f_{d_i|n}(d)\mathbb{P}(n)$$

$$= \sum_{n=S}^{\infty} \frac{n!}{(S-i-1)!(n-S+i)!} \left(\frac{d}{T}\right)^{S-i-1}$$

$$\times \left(\frac{T-d}{T}\right)^{n-S+i} \frac{(\lambda T)^n}{n!} e^{-\lambda T}$$

$$= \frac{\lambda^{S-i} d^{S-i-1}}{(S-i-1)!} e^{-\lambda T} \sum_{n=S}^{\infty} \frac{(\lambda(T-d))^{n-S+i}}{(n-S+i)!}$$

$$= \Gamma_d(S-i,\lambda) \left(1 - \frac{\Gamma_{\text{inc}}(i,\lambda(T-d))}{(i-1)!}\right) \qquad (17)$$

and

(2) If $n < S$:

$$\sum_{n=i}^{S} f_{d_i|n}(d)\mathbb{P}(n) = \sum_{n=i}^{S} \frac{n!}{(n-i)!(i-1)!} \left(\frac{d}{T}\right)^{n-i}$$

$$\times \left(\frac{T-d}{T}\right)^{n-i} \frac{1}{T} \frac{(\lambda T)^n}{n!} e^{-\lambda T}$$

$$= \frac{\lambda^i (T-d)^{i-1}}{(i-1)!} e^{-\lambda T} \sum_{n=i}^{S} \frac{(\lambda d)^{n-i}}{(S-i-1)!}$$

$$= \frac{\lambda^i (T-d)^{i-1}}{(i-1)!} e^{-\lambda(T-d)} \frac{\Gamma_{\text{inc}}(S-i,\lambda d)}{(S-i-1)!}$$

$$= \Gamma_{T-d}(i,\lambda) \frac{\Gamma_{\text{inc}}(S-i,\lambda d)}{(S-i-1)!} \qquad (18)$$

the final probability is the sum of the two components.

□

Similarly to the time-based assembly algorithms, the cases where $i > n$ give null burst-assembly delay. The amount of cases at which this event occurs is given by:

$$\sum_{n=0}^{i-1} \frac{(\lambda T)^n}{n!} e^{-\lambda T} = \frac{\Gamma_{\text{inc}}(i,\lambda T)}{(i-1)!} \qquad (19)$$

Numerical and simulation experiments

This section aims to check the validity of the equations obtained in the previous lemmas with simulated results, and further compare the three burst-assembly algorithms. To this end, we have simulated 2×10^5 packets arriving at a border node at a rate $\lambda = \frac{1}{EX} = 10$ packets per unit of time. We have considered a size-based algorithm with $S_{\max} = 51$ packets, and a time-based algorithm with $T_{\max} = \frac{S_{\max}-1}{\lambda} = 5$ units of time, such that both policies output bursts with the same average size. Finally, a mixed-based algorithm with values $(S_{\max} = 51, T_{\max} = 5)$ has also been simulated.

Figure 2 shows the simulated burst-assembly delay suffered by the 1st, 15th, 30th and 45th packet following the size-based burst-assembly algorithm, together with the theoretical distribution given by Lemma 1. As expected, the theoretical gamma distribution accurately matches each packet's burst assembly delay. Clearly, *the early arrivals (Fig. 2 top-left) experience higher and more variable values of delay than the latter ones (Fig. 2 botton-right)*, as expected from Eqs. 3 and 4.

Figure 3 shows the same metrics but for the time-based assembly algorithm with $T_{\max} = 5$ units of time. Again, the delay values predicted by Lemma 2 agree with the simulation results. It is also interesting to see the fact that, for the ith packet, the larger the value of i, the greater the probability of zero delay given by Eq. 12, that is, the probability of burst sizes smaller than i. Hence, in such cases, the Dirac delta takes a higher value.

Figure 4 shows the burst-assembly delay of the 1st, 15th, 30th and 45th packet under the $(S_{\max} = 51, T_{\max} = 5)$ policy. The figure also shows the burst-formation probability components, as explained in the proof of Lemma 3. Clearly, the total probability density function arises as the weighted sum of such components.

Finally, Fig. 5 shows a comparison of the burst-assembly delay experienced by the 1st, 15th, 30th and 45th packets under the three different strategies. For simplicity, the plot shows the cumulative distribution function (CDF).

As shown, although the size-based assembly policy does not provide a delay bound, the delay CCD exceeds with little probability the value:

$$\frac{S-i}{\lambda} + 3\sqrt{\frac{S-i}{\lambda^2}} \qquad (20)$$

which equals 7.12, 5.4, 3.47 and 1.33 units of time for the 1st, 15th, 30th and 45th packet, respectively. On the other hand, time-based assembly algorithms ensure that no packets experience a burst-assembly delay above the $T_{\max}$ value, which is crucial for packets with strict delay constrains, as shall be shown in the next section. Finally, the mixed size- and time-based strategies shows a combined behaviour of the two strategies, and thus behave similarly to the $T_{\max}$ strategy for early arrivals experiencing high delays and to the $S_{\max}$ strategy for early arrivals experiencing low delay values, and vice-versa.
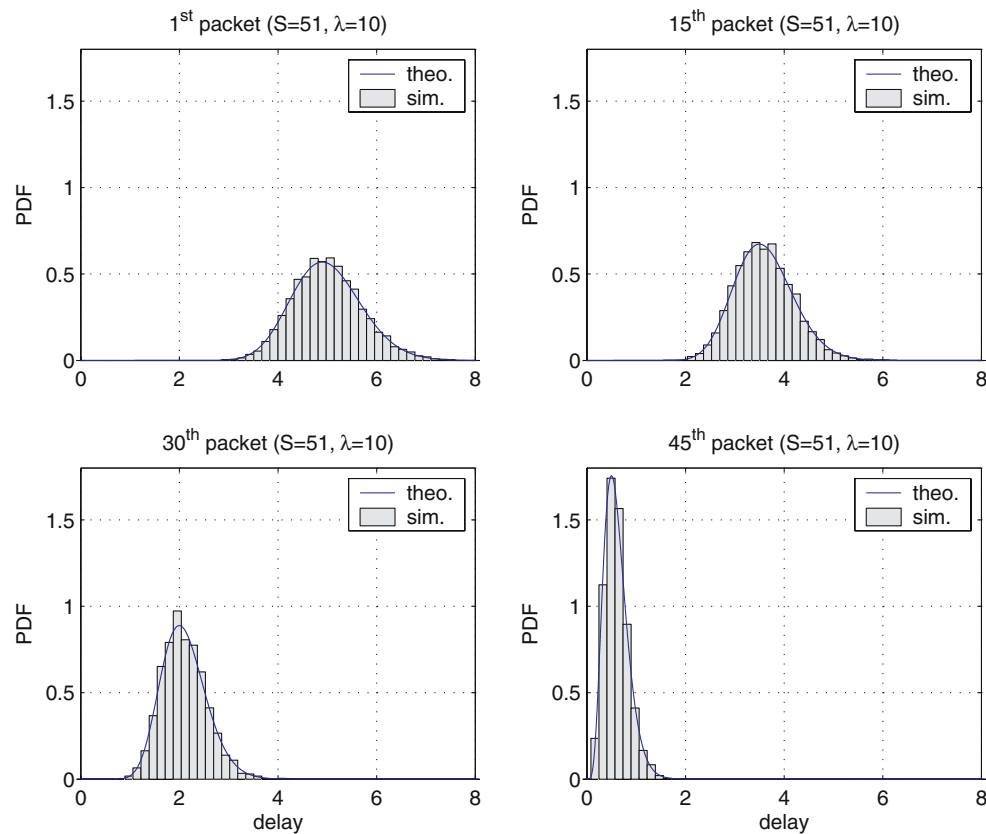
Fig. 2 Delay analysis of the 1st (top-left), 15th (top-right), 30th (bottom-left) and 45th (bottom-right) packet obtained when using a burst-assembly algorithm with $S_{max} = 51$ and $\lambda = 10$

Burst-assembly algorithms with service differentiation

When dealing with delay-based service differentiation, size-based burst-assembly strategies are not very appealing since packets may experience excessive delay values during the burst assembly process. Particularly, in real-time applications such as Internet telephony, videoconferencing, and online gaming, when packets are desired not to suffer excessive delays, the T_{max} burst assembly strategy appears more suitable, since it limits the assembly delay to the so-called T_{max} threshold value.

However, the choice of a small T_{max} value to satisfy such delay-constrained application requirements will typically output optical bursts of small-size, which reduces the benefits of single electrical/optical conversion per burst. Furthermore, since delay-constrained packets typically constitute only a small portion of the total traffic traversing the network, the T_{max} strategy may output small bursts even if no high-priority packets have arrived at the burst assembler. Thus, a small portion of delay-constrained traffic is actually causing that all optical bursts are shaped to meet their requirements, which is obviously very inefficient. Nevertheless, instead of considering a single T_{max} constrain for all

packet arrivals, it makes more sense to use a T_{max} threshold values for each traffic class, in order to ensure that each packet will suffer no longer assembly delays than what is specified by the T_{max} value of its traffic class. Consequently, each packet arrival imposes a maximum burst-formation time, given by its associated T_{max}.

For simplicity, let us consider that input traffic at OBS ingress nodes carry packets from only two different classes of service, namely, the high-priority class and the low-priority class. Additionally, let us further assume that the two classes arrive following a Poissonian basis with λ_h and λ_l input rates and are required not to suffer a delay greater than T_h and T_l, respectively. Typically, $\lambda_l > \lambda_h$ since low-priority packets are more common in practice. Also, $T_l > T_h$, that is, low-priority packets tolerate a higher delay value than high-priority ones.

The following analyses the burst-size distribution obtained when using such (T_l, T_h) burst-assembly strategy. For simplicity, this analysis has been splitted into two cases: in the former, the burst assembler operates on a immediate departure basis after a high-priority packet arrival, that is, the burst is released straight after the first high-priority packet has arrived, i.e., $T_h = 0$; the latter is
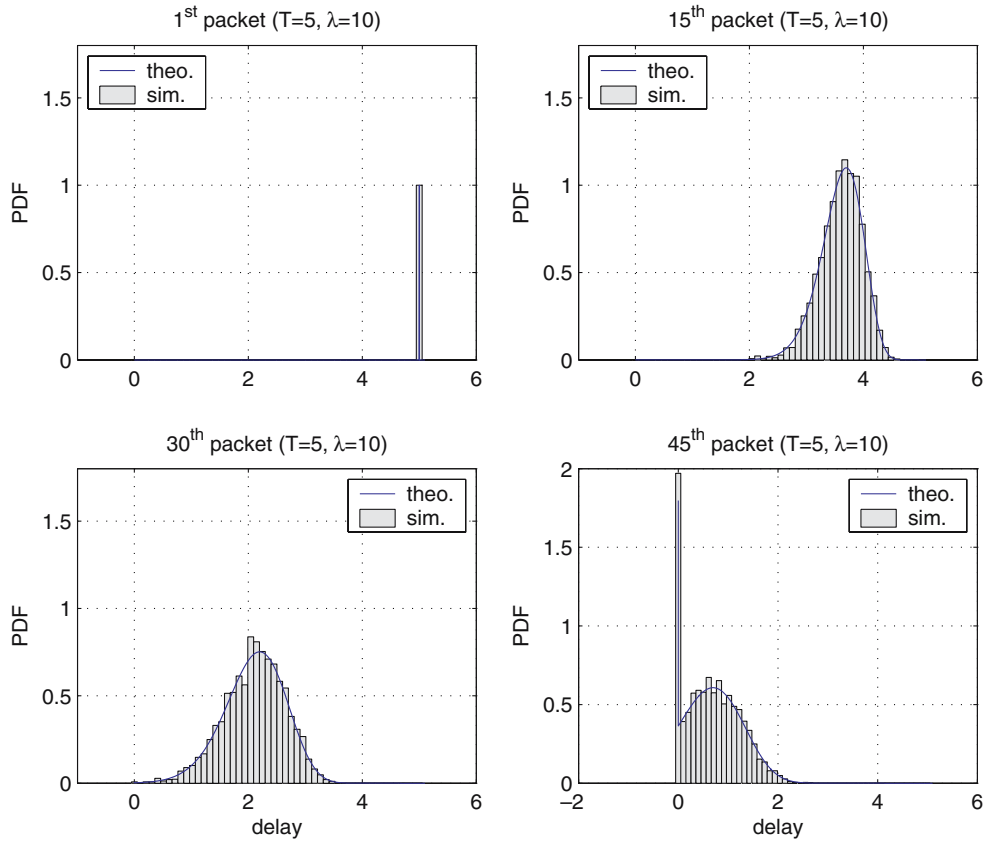
Fig. 3 Delay analysis of the 15th (top-right), 30th (bottom-left) and 45th (bottom-right) packet obtained when using a burst-assembly algorithm with $T_{max} = 5$ and $\lambda = 10$. For the 1st the delay is equal to $T_{max} = 5$ units of time

slightly more complicated since it considers the delayed departure case, that is, when $T_h > 0$.

Burst immediate departure ($T_h = 0$)

This former case assumes $T_h = 0$, that is, as soon as a high-priority packet has arrived at the burstifier, the optical burst is generated straightafter. The analysis of the burst-size distribution requires to take into account the following two possible situations separately: (1) the first packet arrival is of high-priority, thus the burst contains only one packet; (2) the first packet arrival is of low-priority, thus triggering the T_l timer. Clearly, in the second situation, two possible situations may occur, namely: (2a) no high-priority packets arrive before the T_l timer expires, and (2b) at least one high-priority packet arrives within time $[0, T_l]$, say at time $0 < t_h < T_l$. Clearly, the total size distribution hence can be computed as the weighted sum of all cases.

Table 1 summarises all cases, their probabilities and the burst-size distribution arisen in each case. The reader is referred to appendix section "Burst-size distribution with immediate departure ($T_h = 0$)" for the details of how such equations where obtained.

Table 1 Case summary for $T_h = 0$ (inmediate departure)

Case:	$\mathbb{P}(Case)\mathbb{P}(N = n|Case)$
Case 1:	$\frac{\lambda_h}{\lambda_l+\lambda_h}\delta(n)$
Case 2a:	$\frac{\lambda_l}{\lambda_l+\lambda_h}e^{-\lambda_h T_l}\frac{(\lambda_l T_l)^{n-1}}{(n-1)!}e^{-\lambda_l T_l}$
Case 2b:	$\frac{\lambda_l}{\lambda_l+\lambda_h}(1 - e^{-\lambda_h T_l})\frac{\lambda_h}{\lambda_l}\left(\frac{\lambda_l}{\lambda_l+\lambda_h}\right)^{n-1}\frac{\gamma_{inc}(n-1,(\lambda_l+\lambda_h)T_l)}{(n-2)!}$

As shall be shown in the numerical and simulation experiments, this strategy yields small optical bursts when the high-priority packet arrival rate is not much smaller than the low-priority packet arrival rate. A solution to this drawback consists of providing extra time for aggregating packets after a high-priority packet has arrived, i.e., $T_h > 0$. The following section studies this case.

Burst delayed departure ($T_h > 0$)

Again, the analysis of the burst delayed departure model requires the consideration of several other cases: (1) the first packet arrival is of high-priority, thus successive packets are collected for a maximum amount of time
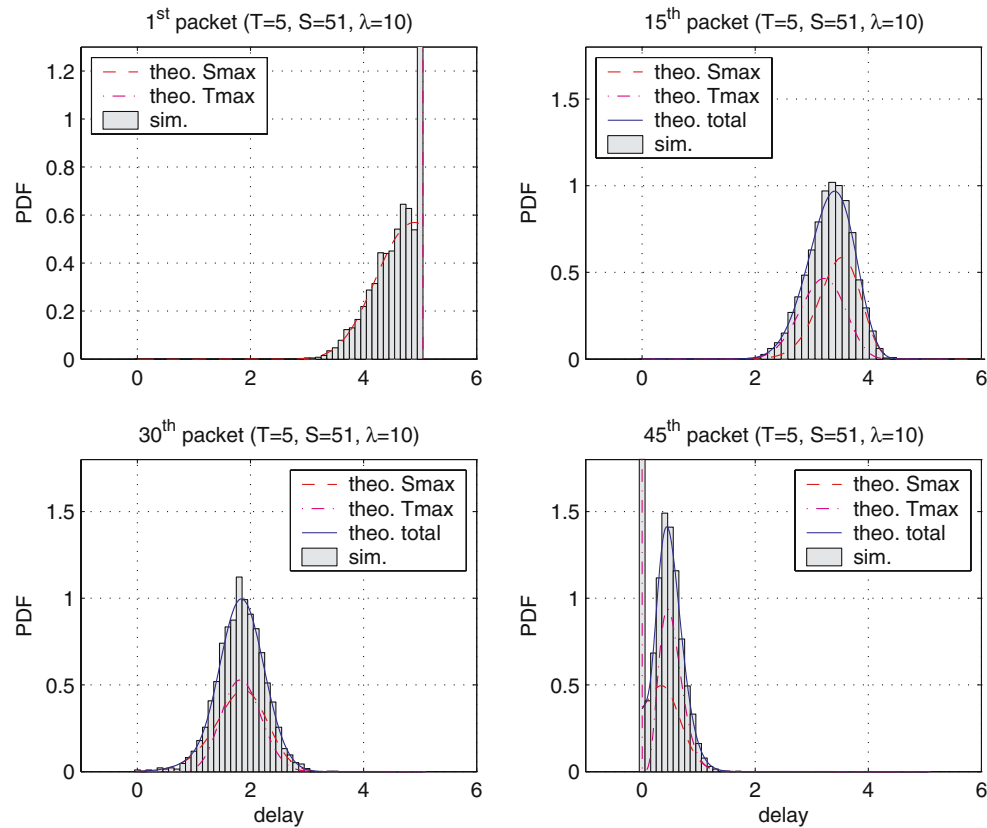
Fig. 4 Delay analysis of the 1st (top-left), 15th (top-right), 30th (bottom-left) and 45th (bottom-right) packets obtained when using a burst-assembly algorithm with $S_{\max} = 51$ and $T_{\max} = 5$ and $\lambda = 10$

given by T_h; (2) the first packet arrival is of low-priority, thus triggering the T_l timer. In the second case, three possible situations may occur, namely: (2a) no high-priority packets arrive before T_l expires; (2b) the first high-priority packet arrives at time $t_h \in [0, T_l - T_h]$, thus setting the burst-assembly timer to the value $t_h + T_h$; and (2c), the first high-priority packet arrives at time $t_h \in [T_l - T_h, T_l]$, hence the burst-assembly timer value remains T_l. Again, the total size distribution can be computed as the weighted sum of all cases.

A summary of the equations obtained is presented in Table 2. Again, the reader is encouraged to refer to appendix section "Burst-size distribution with delayed departure ($T_h > 0$)" for further details.

Numerical and simulation experiments

This section shows the validity of the equations obtained above with simulation experiments. As in the previous numerical example, we have simulated 2×10^5 packet arrivals on a Poissonian basis. The low- and high-priority packet incoming rates considered in the experiments are: ($\lambda_l = 5, \lambda_h = 1$) packets per unit of time. Figure 6 shows the burst-size distribution obtained under

the immediate departure strategy with timing parameters $T_l = 4, T_h = 0$.

Clearly, the theoretical probability density function obtained in the previous section accurately matches the simulated results. In general terms, the immediate departure model outputs small optical bursts, since the optical burst is completed as soon as a high-priority packet arrives, and this situation occurs with probability $\frac{\lambda_h}{\lambda_l + \lambda_h} = \frac{1}{6}$. Thus, the average optical burst can be enlarged just by increasing the value of $T_h > 0$ (delayed departure model).

In the light of this, Fig. 7 shows the results obtained for the delayed departure model, with the same simulation parameters as in the inmediate departure experiment, but with several T_h values, i.e., $T_h = 0$ (top-left), $T_h = 1$ (top-right), $T_h = 2$ (bottom-left) and $T_h = 3$ (bottom-right). Obviously, Fig. 7 (top-left) is the same plot as Fig. 6.

As shown, the average burst-size increases, the larger the value of T_h is. This is obviously expected since a larger value of T_h gives extra time for more packets to be assembled, that is, those packets arriving within time $[t_h, t_h + T_h]$, where $t_h \in [0, T_l]$ refers to the time at which the first high-priority packet arrives at the
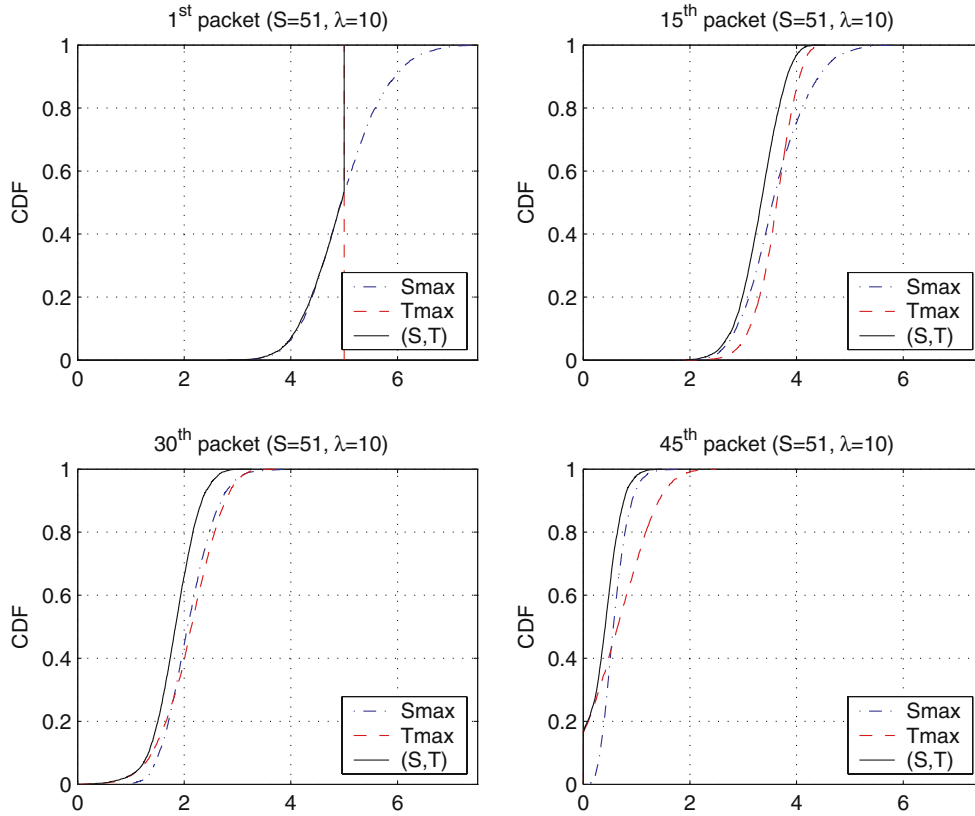
Fig. 5 Cumulative distribution function of the 1st (top-left), 15th (top-right), 30th (bottom-left) and 45th (bottom-right) burst-assembly packet delay obtained with the three burst-assembly algorithms ($S_{\max} = 51$ and $T_{\max} = 5$ and $\lambda = 10$)

Table 2 Case summary for $T_h > 0$ (delayed departure)

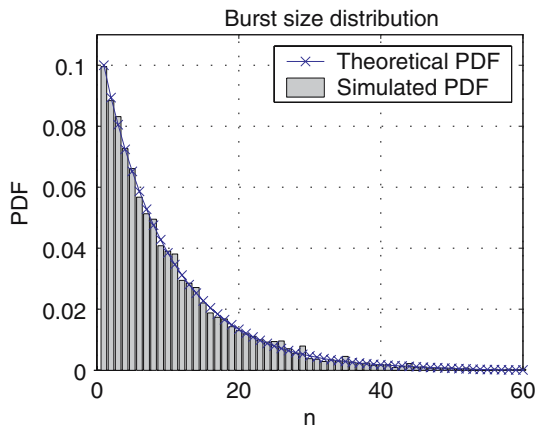| Case:	$\mathbb{P}(Case)\mathbb{P}(N = n\|Case)$
Case 1:	$\frac{\lambda_h}{\lambda_l+\lambda_h} \frac{((\lambda_l+\lambda_h)T_h)^{n-1}}{(n-1)!} e^{-(\lambda_l+\lambda_h)T_h}$
Case 2a:	$\frac{\lambda_l}{\lambda_l+\lambda_h} \frac{(\lambda_l T_l)^{n-1}}{(n-1)!} e^{-(\lambda_l+\lambda_h)T_l}$
Case 2b:	$\frac{\lambda_h}{\lambda_l+\lambda_h} \left(\frac{\lambda_l}{\lambda_l+\lambda_h}\right)^{n-1} e^{\frac{\lambda_h}{\lambda_l}(\lambda_l+\lambda_h)T_h} \frac{\gamma_{\text{inc}}(n-1,(\lambda_l+\lambda_h)(T_l+\frac{\lambda_h}{\lambda_l}T_h))-\gamma_{\text{inc}}(n-1,(\lambda_l+\lambda_h)^2\frac{1}{\lambda_l}T_h)}{(n-2)!}$
Case 2c:	$\frac{\lambda_l}{\lambda_l+\lambda_h} e^{-(\lambda_l T_l+\lambda_h T_l)} \frac{(\lambda_l T_l+\lambda_h T_h)^{n-1}-(\lambda_l T_l)^{n-1}}{(n-1)!}$

Fig. 6 Case example for $T_h = 0$

burst-assembler. In the light of this, Fig. 8 presents the average burst-size and standard deviation for different values of T_h in the range $T_h \in (0, T_l)$. As shown, the burst-size standard deviation maintains, while the average burst-size significantly increases with T_h.

Summary and conclusions

The burst-assembly algorithms employed at OBS border nodes play a crucial role in the analysis and characterisation of OBS networks, for two reasons mainly:

- Burst-assembly algorithms determine the size-structure of outgoing optical bursts, which has a
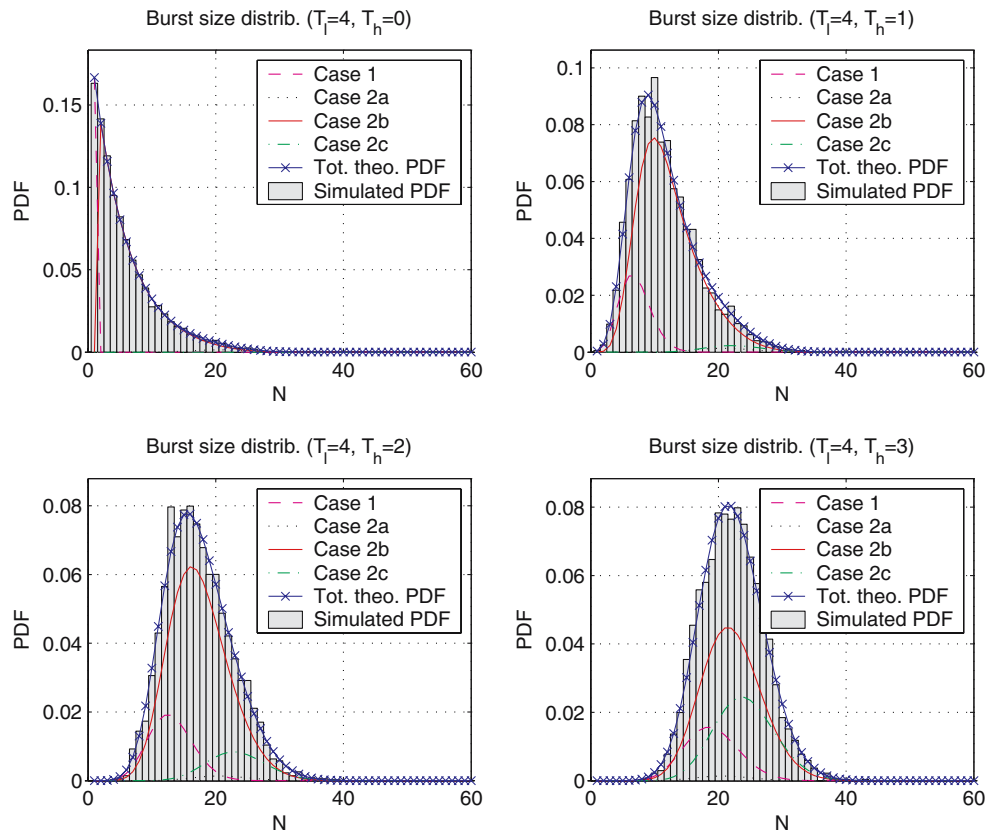
Fig. 7 Case example for $T_h > 0$. $T_h = 0$ (top-left), $T_h = 1$ (top-right), $T_h = 2$ (bottom-left) and $T_h = 3$ (bottom-right)
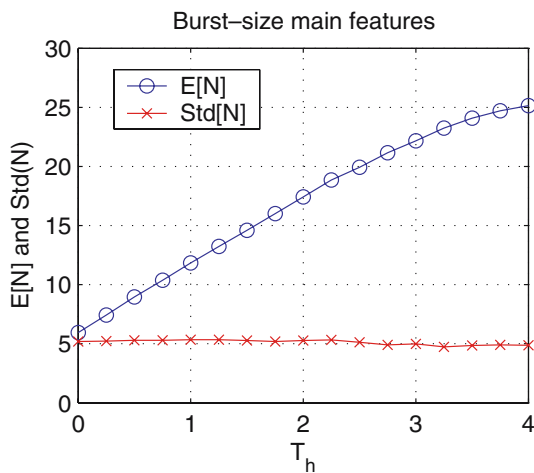

Fig. 8 Mean and standard deviation of burst size for several values of T_h, with parameters ($\lambda_l = 5, \lambda_h = 1$) and $T_l = 4$

further impact on the blocking probability exhibited at intermediate nodes, since the schuduling algorithms have more difficulties in finding available time-slots to allocate them. This impacts on the global operation of the optical network and its performance, via the probability of burst loss.

- Burst-assembly strategies also determine the extra delay given to each packet due to the burstification process. Such delay is given by the burst-assembly strategy employed at the border node and the relative order with respect to other arrivals. This impacts on the performance perceived by the particular application to which such packet belongs to.

While the former cause–effect relationship has been extensively analysed by the research community, the second has not been considered that much.

This work has analysed and provided a detailed study on the burst-assembly delay suffered by each packet in a burst, assuming the most typical burst-assembly techniques found in the literature.

Additionally, since such delay may be excessive for certain applications, this work proposes a new burst-assembly algorithm which provides quality of service differentiation at the burst-assembly process level. This is achieved by categorising packets into two or more priority-levels and permitting the high-priority packets control and modify the burst-assembly process. The burst-size distribution assuming different input rates and burst-release timings is also obtained. It is worth

noting that by combining high- and low-priority packets into the same burst a larger burst size is obtained. This effect is beneficial for the switch implementation, as the switching time requirements are relaxed. Furthermore, we also note that our scheme can be used in combination with burst segmentation schemes at the core OBS switches. By adequately placing packets either at the burst head or tail, a different packet drop probability can be obtained. This scheme is called Optical Composite Burst Switching [6]. We further remark that our delay calculations also apply if such scheme is adopted, since the burst assembly delay is dominated by the arrival times of the packets that make up a burst. Then, packets may be reordered within a burst, but this process does not affect much the packet delay at the edge, i.e., the interval between the packet arrival and the time epoch the burst is ready for departure.

Such service differentiation at the burst-assembly level permits delay-based quality-of-service support and guaranteed delay bounds between the border nodes of the optical network, since no queuing delay exists in OBS networks. This permits different treatment to packets with delay constrains over an underlying OBS-based network.

Appendix

Burst-assembly process revisited

The following lemma states the conditional burst-assembly delay PDF of packet i, as stated in Lemma 2:

Lemma 4 *Let $n = 1, 2 \ldots$ refer to the number of packets arriving at the burstifier in the time interval $(0, T_{\max})$. Then, the ith arrival experiences the following delay distribution function, conditioned to n packet arrivals within $(0, T_{\max})$:*

$$f_{d_i|n}(d) = \frac{n!}{(n-i+1)!(i-2)!} \frac{1}{T} \left(\frac{d}{T}\right)^{n-i+1} \left(\frac{T-d}{T}\right)^{i-1},$$
$$0 \leq d \leq T_{\max}, \quad i \leq n \quad (21)$$

Proof Since the arrivals occur following a Poissonian basis, the arrival times are uniformly distributed within the interval $(0, T_{\max})$. Then, the ith packet arrival time is given by the ith order statistic of a uniform random variable in $(0, T_{\max})$ [4, see chapter 2]. Let us thus refer to such arrival time by $a_{(i)}$, with PDF $f_{a_{(i)}}(d), 0 \leq d \leq T_{\max}$. Then $f_{d_i|n}(d) = f_{a_{(i)}}(T-d)$ and the lemma is proved. □

Burst-size distribution with immediate departure $(T_h = 0)$

This section derives the equations shown in Table 1. To do so, we shall consider each case separately.

Case 1: first packet of high-priority ($p_1 = h$)

Clearly, if the first packet arriving is of high-priority, then the optical burst only contains a single packet, i.e., $P(N = n|p_1 = h) = \delta(n)$. This case occurs with probability $\frac{\lambda_h}{\lambda_l + \lambda_h}$.

Case 2a: first packet of low priority ($p_1 = l$) and no high-priority packet arrivals within time $[0, T_l]$ ($N_h = 0$)

This case occurs with probability $\frac{\lambda_l}{\lambda_l + \lambda_h} e^{-\lambda_h T_l}$. The former term states the probability of the first packet to be of low priority, whereas the second gives the probability of no high-priority packets within time $[0, T_l]$. The resulting burst size distribution is given by the amount of packets arriving within time $[0, T_l]$, that is:

$$P(N = n|(p_1 = l) \cap (N_h = 0)) = \frac{(\lambda_l T_l)^{n-1}}{(n-1)!} e^{-\lambda_l T_l} \quad (22)$$

Case 2b: first packet of low priority ($p_1 = l$) and at least one high-priority packet arrival within time $[0, T_l]$ ($N_h > 0$)

Finally, this case occurs with probability $\frac{\lambda_l}{\lambda_l + \lambda_h}(1 - e^{-\lambda_h T_l})$. The size of the outgoing burst obviously depends on the moment t_h at which the high-priority packet arrives. Clearly, such $t_h \in [0, T_l]$. As shown in appendix section "Burst-assembly process revisited" the time t_h is distributed as the first order statistic of a uniform random variable in the range $[0, T_l]$. Computing the size distribution of this case requires to take into account the probability of N_h high-priority packets arrivals within time $[0, T_l]$, along with the time t_h at which the first high-priority packet arrival occurs. That is:

$$P(N = n|(p_1 = l) \cap (N_h > 0))$$
$$= \sum_{j=1}^{\infty} P(N = n|N_h = j) P(N_h = j)$$
$$= \sum_{j=1}^{\infty} \left(\int_0^{T_l} \frac{(\lambda_l t_h)^{n-2}}{(n-2)!} e^{-\lambda_l t_h} \left(\frac{T_l - t_h}{T_l}\right)^{j-1} \frac{j}{T_l} dt_h \right) \frac{(\lambda_h T_l)^j}{j!} e^{-\lambda_h T_l}$$
$$= \int_0^{T_l} \frac{(\lambda_l t_h)^{n-2}}{(n-2)!} e^{-\lambda_l t_h} \left(\sum_{j=1}^{\infty} \left(\frac{T_l - t_h}{T_l}\right)^{j-1} \frac{j}{T_l} \frac{(\lambda_h T_l)^j}{j!} e^{-\lambda_h T_l} \right) dt_h$$

$$= \int_0^{T_l} \frac{(\lambda_l t_h)^{n-2}}{(n-2)!} e^{-\lambda_l t_h} \left(\lambda_h \sum_{j=1}^{\infty} \frac{(\lambda_h(T_l - t_h))^{j-1}}{(j-1)!} e^{-\lambda_h T_l} \right) dt_h$$

$$= \int_0^{T_l} \frac{(\lambda_l t_h)^{n-2}}{(n-2)!} e^{-\lambda_l t_h} \left(\lambda_h e^{\lambda_h(T_l - t_h)} e^{-\lambda_h T_l} \right) dt_h$$

$$= \lambda_h \int_0^{T_l} \frac{(\lambda_l t_h)^{n-2}}{(n-2)!} e^{-(\lambda_l + \lambda_h) t_h} dt_h \quad (23)$$

Using the transformation $z = (\lambda_h + \lambda_l) t_h$, Eq. 23 yields:

$$P(N = n | (p_1 = l) \cap (N_h > 0))$$
$$= \frac{\lambda_h}{\lambda_l} \left(\frac{\lambda_l}{\lambda_l + \lambda_h} \right)^{n-1} \int_0^{(\lambda_l + \lambda_h) T_l} z^{n-2} e^{-z} dz$$
$$= \frac{\lambda_h}{\lambda_l} \left(\frac{\lambda_l}{\lambda_l + \lambda_h} \right)^{n-1} \frac{\gamma_{\text{inc}}(n-1, (\lambda_l + \lambda_h) T_l)}{(n-2)!} \quad (24)$$

where γ_{inc} refers to the lower incomplete gamma function.[2]

Burst-size distribution with delayed departure ($T_h > 0$)

This section derives the equations given in Table 2. Again, we shall consider each case separately.

Case 1: first packet of high-priority ($p_1 = h$)

Again, as in the case of immediate departure, this case occurs with probability $\frac{\lambda_h}{\lambda_l + \lambda_h}$. However, the size of the outgoing bursts is not one since the timer $T_h > 0$ permits more packet arrivals. Such amount of packets arriving within time $[0, T_h]$ with a total input rate of $\lambda_l + \lambda_h$ is given by:

$$P(N = n | (p_1 = h)) = \frac{((\lambda_l + \lambda_h) T_h)^{n-1}}{(n-1)!} e^{-(\lambda_l + \lambda_h) T_h} \quad (25)$$

Case 2a: first packet of low priority ($p_1 = l$) and no high-priority packet arrivals after it ($N_h = 0$)

This case occurs with probability $\frac{\lambda_l}{\lambda_l + \lambda_h} e^{-\lambda_h T_l}$ and the resulting optical bursts have the following size distribution:

$$P(N = n | (p_1 = l) \cap (N_h = 0)) = \frac{(\lambda_l T_l)^{n-1}}{(n-1)!} e^{-\lambda_l T_l} \quad (26)$$

Case 2b: first packet of low priority ($p_1 = l$) and first high-priority packet arriving within time $t_h \in [0, T_l - T_h]$

This case occurs with probability $\frac{\lambda_l}{\lambda_l + \lambda_h}$. Let N_h refer to the number of high-priority packets arriving withing time $[0, T_l - T_h]$ and $t_h \in (0, T_l - T_h)$ the moment at which the first high-priority packet arrives. Thus, the

number of packets arriving within time $(0, T_h)$ is characterised by a Poisson distribution with rate $\lambda_l t_h$ and the number of packets arriving within time $(t_h, t_h + T_h)$ is given by a Poisson distribution with rate $(\lambda_l + \lambda_h) T_h$. The distribution of t_h is given by the first order statistic of a uniform random variable in the range $(0, T_l - T_h)$ assuming N_h high-priority packet arrivals. The burst size distribution in this case is thus given by:

$$P(N = n | (p_1 = l) \cap (N_h > 0) \cap (t_h \in (0, T_l - T_h)))$$
$$= \sum_{j=1}^{\infty} P(N = n | N_h = j) P(N_h = j)$$
$$= \sum_{j=1}^{\infty} \left(\int_0^{T_l - T_h} \frac{(\lambda_l t_h + (\lambda_l + \lambda_h) T_h)^{n-2}}{(n-2)!} \right.$$
$$\times e^{-(\lambda_l t_h + (\lambda_l + \lambda_h) T_h)} \left(\frac{T_l - T_h - t_h}{T_l - T_h} \right)^{j-1} \frac{j}{T_l - T_h} dt_h \Bigg)$$
$$\times \frac{(\lambda_h(T_l - T_h))^j}{j!} e^{-\lambda_h(T_l - T_h)}$$
$$= \int_0^{T_l - T_h} \frac{(\lambda_l t_h + (\lambda_l + \lambda_h) T_h)^{n-2}}{(n-2)!}$$
$$\times e^{-(\lambda_l t_h + (\lambda_l + \lambda_h) T_h)} dt_h \left(\sum_{j=1}^{\infty} \left(\frac{T_l - T_h - t_h}{T_l - T_h} \right)^{j-1} \right.$$
$$\times \frac{j}{T_l - T_h} \frac{(\lambda_h(T_l - T_h))^j}{j!} e^{-\lambda_h(T_l - T_h)} \Bigg) dt_h$$
$$= \int_0^{T_l - T_h} \frac{(\lambda_l t_h + (\lambda_l + \lambda_h) T_h)^{n-2}}{(n-2)!} e^{-(\lambda_l t_h + (\lambda_l + \lambda_h) T_h)}$$
$$\times \left(\lambda_h \sum_{j=1}^{\infty} (\frac{(\lambda_h(T_l - T_h - t_h))^{j-1}}{(j-1)!} e^{-\lambda_h(T_l - T_h)} \right) dt_h$$
$$= \int_0^{T_l - T_h} \frac{(\lambda_l t_h + (\lambda_l + \lambda_h) T_h)^{n-2}}{(n-2)!}$$
$$\times e^{-(\lambda_l t_h + (\lambda_l + \lambda_h) T_h)} \left(\lambda_h e^{-\lambda_h t_h} \right) dt_h$$
$$= \lambda_h \int_0^{T_l - T_h} \frac{(\lambda_l t_h + (\lambda_l + \lambda_h) T_h)^{n-2}}{(n-2)!}$$
$$\times e^{-((\lambda_l + \lambda_h) t_h + (\lambda_l + \lambda_h) T_h)} dt_h \quad (27)$$

Using the transformation $t_h = \frac{z}{\lambda_l + \lambda_h} - \frac{\lambda_l + \lambda_h}{\lambda_l} T_h$, Eq. 27 yields:

$$P(N = n | (p_1 = l) \cap (N_h > 0) \cap (t_h \in (0, T_l - T_h)))$$
$$= \lambda_h \int_{\frac{(\lambda_l + \lambda_h)^2}{\lambda_l} T_h}^{(\lambda_l + \lambda_h)(T_l + \frac{\lambda_h}{\lambda_l} T_h)} \frac{\left(\frac{\lambda_l}{\lambda_l + \lambda_h} z \right)^{n-2}}{(n-2)!}$$
$$\times e^{-(z - \frac{(\lambda_l + \lambda_h)^2}{\lambda_l} T_h + (\lambda_l + \lambda_h) T_h)} \frac{dz}{\lambda_l + \lambda_h}$$

---

[2] Lower incomplete gamma function $\gamma_{\text{inc}}(n, x) = \int_0^x z^{n-1} e^{-z} dz$.

$$= \frac{\lambda_h}{\lambda_l + \lambda_h} \left(\frac{\lambda_l}{\lambda_l + \lambda_h} \right)^{n-2} \frac{e^{\frac{\lambda_h}{\lambda_l}(\lambda_l + \lambda_h) T_h}}{(n-2)!}$$
$$\times \left(\gamma_{\text{inc}} \left(n-1, (\lambda_l + \lambda_h) \left(T_l + \frac{\lambda_h}{\lambda_l} T_h \right) \right) \right.$$
$$\left. - \gamma_{\text{inc}} \left(n-1, \frac{(\lambda_l + \lambda_h)^2}{\lambda_l} T_h \right) \right) \qquad (28)$$

Case 2c: first packet of low priority ($p_1 = l$) and first high-priority packet arriving within time
$t_h \in [T_l - T_h, T_h]$

This case occurs with probability $\frac{\lambda_l}{\lambda_l + \lambda_h}$. Again, let N_h refer to the number of high-priority packets arriving withing time $[0, T_l - T_h]$, and $t_h \in (T_l - T_h, T_l)$ the time at which the first of such high-priority packets arrives. The number of packets arriving within time $(0, t_h)$ are charecterised by a Poisson distribution with rate $\lambda_l t_h$, whereas the number of packets arriving withing time t_h, T_l are characterised by a Poisson distribution with rate $(\lambda_l + \lambda_h)(T_l - t_h)$. Thus, the size distribution is given by:

$$P(N = n | (p_1 = l) \cap (N_h > 0) \cap (t_h \in (T_l - T_h, T_l)))$$
$$= \sum_{j=1}^{\infty} P(N = n | N_h = j) P(N_h = j)$$
$$= \sum_{j=1}^{\infty} \left(\int_{T_l - T_h}^{T_l} \frac{(\lambda_l t_h + (\lambda_l + \lambda_h)(T_l - t_h))^{n-2}}{(n-2)!} \right.$$
$$\left. \times e^{-(\lambda_l t_h + (\lambda_l + \lambda_h)(T_l - t_h))} \left(\frac{T_l - t_h}{T_h} \right)^{j-1} \frac{j}{T_h} dt_h \right)$$
$$\times \frac{(\lambda_h T_h)^j}{j!} e^{-\lambda_h T_h}$$
$$= \int_{T_l - T_h}^{T_l} \frac{(\lambda_l t_h + (\lambda_l + \lambda_h)(T_l - t_h))^{n-2}}{(n-2)!}$$
$$\times e^{-(\lambda_l t_h + (\lambda_l + \lambda_h)(T_l - t_h))} dt_h$$
$$\times \left(\sum_{j=1}^{\infty} \left(\frac{T_l - t_h}{T_h} \right)^{j-1} \frac{j}{T_h} \frac{(\lambda_h T_h)^j}{j!} e^{-\lambda_h T_h} \right) dt_h$$
$$= \int_{T_l - T_h}^{T_l} \frac{(\lambda_l t_h + (\lambda_l + \lambda_h)(T_l - t_h))^{n-2}}{(n-2)!}$$
$$\times e^{-(\lambda_l t_h + (\lambda_l + \lambda_h)(T_l - t))}$$
$$\times \left(\lambda_h \sum_{j=1}^{\infty} \frac{(\lambda_h (T_l - t_h))^{j-1}}{(j-1)!} e^{-\lambda_h T_h} \right) dt_h$$
$$= \int_{T_l - T_h}^{T_l} \frac{(\lambda_l t_h + (\lambda_l + \lambda_h)(T_l - T_h))^{n-2}}{(n-2)!}$$
$$\times e^{-(\lambda_l t_h + (\lambda_l + \lambda_h)(T_l - T_h))} \left(\lambda_h e^{-\lambda_h (t_h + T_h - T_l)} \right) dt_h$$

$$= \lambda_h \int_{T_l - T_h}^{T_l} \frac{(\lambda_l t_h + (\lambda_l + \lambda_h)(T_l - T_h))^{n-2}}{(n-2)!}$$
$$\times e^{-(\lambda_l T_l + \lambda_h T_h)} dt_h$$
$$= \frac{e^{-(\lambda_l T_l + \lambda_h T_h)}}{(n-1)!} \left((\lambda_l T_l + \lambda_h T_h)^{n-1} - (\lambda_l T_l)^{n-1} \right). \quad (29)$$

References

[1] Cao, X. et al. (2002). Assembling TCP/IP packets in Optical Burst Switched networks. In: *Proceedings of IEEE GLOBECOM, Taipei, Taiwan*, vol. 3 (pp. 2808–2812)

[2] Choi, J.Y. et al. (2004). *The effect of burst assembly on performance of Optical Burst Switched networks*. Lecture notes in Computer Science, vol. 3090 (pp. 729–739)

[3] Choi, J. Y., Choi, J. S., & Kang, M. (2005). Dimensioning burst assembly process in Optical Burst Switching networks. *IEICE Transactions of Communications, E88-B*(10), 3855–3863

[4] David, H.A. (1981). *Order statistics*. New York: John Wiley & Sons, Inc.

[5] de Vega Rodrigo, M., & Gotz, J.: (2004). An analytical study of Optical Burst Switching aggregation strategies. In: *Proceedings of Broadnets, (Workshop on OBS), San Jose, California*

[6] Detti, A., Eramo, V., & Listanti, M. (2002). Performance evaluation of a new technique for IP support in a WDM optical network: Optical Composite Burst Switching (OCBS). *IEEE/OSA Journal of Lightwave Technology, 20*(2), 154–165

[7] Dolzer, K., & Gauger, C. (2001) On burst assembly in Optical Burst Switching networks—a performance evaluation of Just-Enough-Time. In: *Proceedings of the 17th International Telegraffic Congress* (pp. 149–160)

[8] Ge, A., Callegati, F., & Tamil, L. S. (2000). On optical burst switching and self-similar traffic. *IEEE Communication Letters, 4*(3), 98–100

[9] Haga, P. et al. (2006). Understanding packet pair separation beyond the fluid model: the key role of traffic. In: *Proceedings of IEEE INFOCOM Barcelona, Spain*

[10] Iizuka, M. et al. (2002). A scheduling algorithm minimizing voids generated by arriving bursts in Optical Burst Switched WDM networks. In: *Proceedings of IEEE GLOBECOM, Taipei, Taiwan*, vol. 3 (pp. 2736–2740)

[11] Izal, M., & Aracil, J. (2002). On the influence of self-similarity on optical burst switching traffic. In: *Proceedings of IEEE GLOBECOM, Taipei, Taiwan*, vol. 3 (pp. 2308–2312)

[12] Karagiannis, T. et al. (2004). A nonstationary Poisson view of Internet traffic. In: *Proceedings of IEEE INFOCOM, Hong Kong, PRC*, vol. 3 (pp. 1558–1569)

[13] Klinkowski, M. et al. (2005). Impact of burst length differentiation on QoS performance in OBS networks. In: *Proceedings of ICTON, Barcelona, Spain, vol, 1* (pp. 91–94)

[14] Leavens, K. (2002). Traffic characteristics inside optical burst switching networks. In: *Proceedings of SPIE/IEEE OPTICOMM, Boston, Massachusetts*

[15] Liu, J., & Ansari, N. (2004). The impact of the burst assembly interval on the OBS ingress traffic characteristics and system performance. In: *Proceedings of IEEE ICC, Paris, France*, vol. 3 (pp. 1559–1563)

[16] Qiao, C., & Yoo, M. (1999). Optical burst switching (OBS)—A new paradigm for an optical Internet. *Journal of High-Speed Networks, 8*(1), 69–84

[17] Vokkarane, V.M. et al. (2002). Generalized burst assembly and scheduling techniques for QoS support in Optical Burst-Switched networks. In: *Proceedings of IEEE GLOBECOM, Taipei, Taiwan*, vol. 3 (pp. 2747–2751)

[18] Vokkarane, V., Haridoss, K., & Jue, J.P. (2002). Threshold-based burst assembly policies for QoS support in optical burst-switched networks. In: *Proceedings of SPIE/IEEE OPTICOMM, Boston, Massachusetts* (pp. 125–136).

[19] Xiong, M., Vandenhoute, Y., & Cankaya, H. C. (2000) Control architecture in optical burst switched WDM network. *IEEE JSAC, 18*(10), 1838–1851

[20] Xu, L., Perros, H. G., & Rouskas, G. (2001). Techniques for optical packet switching and optical burst switching. *IEEE Communication Magazine, 39*(1), 136–142

[21] Yu, X., Chen, Y., & Qiao, C. (2002). Study of traffic statistics of assembled burst traffic in optical burst switched networks. In: *Proceedings of SPIE/IEEE OPTICOMM, Boston, Massachusetts* (pp. 149–159).

[22] Yu, X., Chen, Y., & Qiao, C. (2002). Performance evaluation of Optical Burst Switching with assembled burst traffic input. In: *Proceedings of IEEE GLOGECOM, Taipei, Taiwan*, vol. 3 (pp. 730–731)

[23] Yu, X. et al. (2003). Performance evaluation of TCP implementations in OBS networks, Tech. Rep. 2003-13, CSE Department, SUNY Buffalo, NY

[24] Yu, X. et al. (2004). Traffic statistics and performance evaluation in Optical Burst Switching networks. *IEEE/OSA Journal of Lightwave Technology, 22*(12), 2722–2738

[25] Zapata, A., & Bayvel, P.: Impact of burst aggregation schemes on delay in Optical Burst Switched networks. In: *Proc. IEEE/LEOS Annual Meeting, Tucson, Arizona* (pp. 57–58)

[26] Zhang, Q. et al. (2005). Analysis of TCP over Optical Burst-Switched Networks with burst retransmission. In: *Proceedings of IEEE GLOBECOM*, vol. 4 St. Louis, MO

J Aracil Javier Aracil received the M.Sc. and Ph.D. degrees (Honors) from Technical University of Madrid in 1993 and 1995, both in Telecommunications Engineering. In 1995 he was awarded with a fulbright scholarship and was appointed as a postdoctoral researches of the department of Electrical Engineering and Computer Sciences, University of California, Berkeley. In 1998 he was a research scholar at the Center for Advanced Telecommunications, Systems and Services of The University of Texas at Dallas. He has been an associate professor for University of Cantabria and Public University of Navarra and he is currently a full professor at Universidad Autónoma de Madrid, Madrid, Spain. His research interest are in optical networks and performance evaluation of communication networks. He has authored more than 50 papers in international conferences and journals. His email address is Javier.Aracil@uam.es

V Lopez Victor López completed his MSc. degree in Telecommunications Engineering with Honours at Universidad de Alcalá in 2005. Before that in 2004, he joined Telefonica Investigacion y Desarrollo where as a researcher in next generation networks for metro, core and access. During this period, he participated in several European Union projects (NOBEL, MUSE, MUPBED) focused in the previous topics. In 2006, he joined the Networking Research Group of Universidad Autónoma de Madrid as a researcher in ePhoton/One Plus Network of Excelence. His research interests are focused on the analysis and characterization of services, design and performance evaluation of traffic monitoring equipment, and the integration of Internet sevices over WDM networks, mainly OBS solutions. His email address is Victor.Lopez@uam.es

J A Hernandez José Alberto Hernández completed the five-year degree in Telecommunications Engineering at Universidad Carlos III de Madrid (Spain) in 2002, and the Ph.D. degree in Computer Science at Loughborough University (United Kingdom) in 2005. After this, he joined the Networking Research Group at Universidad Autónoma de Madrid (Spain), where he actively participates in a number of both national and european research projects concerning the modeling and performance evaluation of communication networks, and particularly the optical burst switching technology. His research interests include the areas at which mathematical modeling and computer networks overlap. His email address is Jose.Hernandez@uam.es

J L deVergara Jorge E. López de Vergara is currently an associate professor in the Computer Science Department of the Universidad Autónoma de Madrid. He received his M.Sc. degree in telecommunications from the Technical University of Madrid in 1998 and finished his Ph.D. in telematics engineering at the same university in 2003, where he held a research grant. He has participated in several spanish and EU research projects. His current research topics include network, service, and distributed application management, focusing on high bandwidth optical networks. His email address is Jorge.Lopez_Vergara@uam.es